Numerical Analysis of Flame Acceleration and Onset of Detonation in Homogenous and Inhomogeneous Mixture

Reza Khodadadi Azadboni[1], Ali Heidari[1] and Jennifer X Wen[2,3]
[1]School of Mechanical & Automotive Engineering, Kingston University London, SW15 3DW, UK

[2] Warwick FIRE, School of Engineering, University of Warwick, Coventry, CV4 7AL, UK

Abstracts

Numerical investigations have been conducted for flame acceleration and transition to detonation in a horizontal obstructed channel with 60 percent blockage ratio filled with hydrogen/air mixture. Both homogeneous and inhomogeneous hydrogen/air mixtures have been considered. The later has a vertical concentration gradient. The density-based solver within the OpenFOAM CFD toolbox developed by the present authors [1] is used. High-resolution grids are facilitated by using adaptive mesh refinement technique, which leads to 30 grid points per half reaction length (HRL) in the finest region near the flame and shock fronts. The forward and backwards jets which represent Richtmyer–Meshkov (RM) instability, were found to impact on the shock front, resulting in the appearance of a secondary triple point on the initial Mach stem on the flame front. Moreover, since both the forward and backwards jet propagates in the shear layer, some small vortices can be found on the surface of the secondary shear layer, which represents the Kelvin-Helmholtz (KH) instability. Additionally, it has been found that the inhomogeneous mixtures cause higher shock and flame velocities compared to the homogeneous mixtures concentration. Also, for both homogenous and inhomgenous mixtures with 30% hydrogen concentration, the onset of detonation occurs within the obstructed channel section, but the homogeneous mixtures show slightly faster flame acceleration and earlier onset.

Keywords: Flame Acceleration, Detonation, DDT, instability, Numerical, Hydrogen

[3]Jennifer.wen@warwick.ac.uk
Correspondence to: Jennifer.Wen@warwick.ac.uk

1. Introduction

Flame acceleration (FA) in obstructed channels have been studied by numerous investigators [e.g. 2,3]. Frolov [4] provided a detailed summary of the acceleration of the Deflagration-to-Detonation Transition (DDT) in gases. DDT in obstructed channels has been studied numerically by Gamezo et al. [5]. Kuznetsov et al. [6] carried out large-scale tests of DDT in an obstructed semi-confined flat layer of stratified hydrogen-air mixture. They also studied the effects of the maximum hydrogen concentration at the top and a vertical concentration gradient on the flame propagation regimes were investigated to derive critical conditions for sonic flame propagation and detonation onset. They found that steeper hydrogen gradients can lead to more reactive mixtures and higher maximum hydrogen concentrations at the top of the layer, which can enable the flame to accelerate to sonic speed. They showed that flame acceleration in mixtures with concentration gradients might be determined by the maximum local hydrogen concentration in semi-confined geometries. Vollmer et al. [7] and Boeck et al. [8] reported that a strong positive effect of concentration gradients could be found on FA, especially in a channel without obstructions. In other words, concentration gradients can result in significantly stronger FA compared to the homogeneous mixtures. Boeck et al. [8] also showed that the FA was stronger in the presence of the gradients. DDT was also observed as reflected shock waves interacting with the deflagration front.

2. Numerical Model

The density-based numerical code (VCEFoam) previously developed by the authors is used [1]. The solver is based on the open source computational fluid dynamic (CFD) toolbox OpenFOAM [9]. The Harten–Lax–van Leer–Contact (HLLC) scheme with multidimensional slope limiters ("cellMDLimited") is used for accurate shock capturing. Compressible Navier–Stokes equations with a chemical reaction mechanism [9] are solved and for turbulence modelling the Monotone Integrated Large Eddy Simulation (MILES) technique is adopted. Further details of VCEFoam and its validations can be found in our previous publications [1, 11,12].

3. The Results

Predictions of cellular detonation

A two-dimensional test case has been selected to examine the capability of VCEFoam in capturing the cellular detonation structures. The schematic of the rectangular domain is shown in Figure *1*. High pressure ($1000 \times p_0$ (atm)) and temperature perturbation ($25 \times T_0$ (K)) were initiated to trigger the detonation waves in the red regions. All four sides of the domain were assumed to have a wall with no-slip boundary conditions.

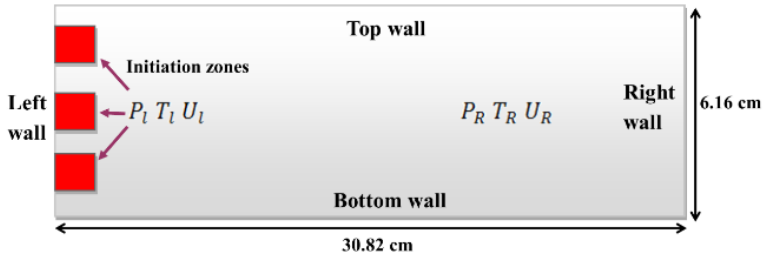

Figure 1. Schematic of the two-dimensional rectangular channel

As mentioned previously, the mesh resolution has a significant impact in capturing the details of the detonation structure as well as having a direct relation with the induction length. The induction time in the unburned combustible mixture is τ_i≈119 μs, and the induction length is L_i≈1.3 mm. In this test case, the grid resolution is 0.065 mm, providing 20 points in the induction length. The maximum Courant number has been set to 0.15. The Marinov [13] hydrogen/air reaction mechanism is used.

Table 1: H2/Air reaction mechanism (Marinov, [13])[units: s, mol, cm3, cal and K].

Reaction	A	b	Ea
(1) $OH + H2 \rightleftarrows H + H_2O$	2.14E+08	1.52	3449.0
(2) $O + OH \rightleftarrows O_2 + H$	2.02E+14	-0.4	0.0
(3) $O + H_2 \rightleftarrows OH + H$	5.06E+04	2.67	6290.0
(4) $H + O_2(+M) \rightleftarrows HO_2(+M)$	4.52E+13	0.0	0.0
low	1.05E+19	-1.257	0.0
(5) $H + O_2(+N_2) \rightleftarrows HO_2(+N_2)$	4.52E+13	0.0	0.0
low	2.03E+20	-1.59	0.0
(6) $H + O_2(+H_2) \rightleftarrows HO_2(+H_2)$	4.52E+13	0.0	0.0
low	1.52E+19	-1.133	0.0
(7) $H + O_2(+H_2O) \rightleftarrows HO_2(+H_2O)$	4.52E+13	0.0	0.0
low	2.10E+23	-2.437	0.0
(8) $OH + HO_2 \rightleftarrows H_2O + O_2$	2.13E+28	-4.827	3500.0
(8b) $OH + HO_2 \rightleftarrows H_2O + O_2$	9.10E+14	0.0	10964.0
(9) $H + HO_2 \rightleftarrows OH + OH$	1.50E+14	0.0	1000.0
(10) $H + HO_2 \rightleftarrows H_2 + O_2$	8.45E+11	0.65	1241.0
(11) $H + HO_2 \rightleftarrows O + H_2O$	3.01E+13	0.0	1721.0
(12) $O + HO_2 \rightleftarrows O_2 + OH$	3.25E+13	0.0	0.0
(13) $OH + OH \rightleftarrows O + H_2O$	3.57E+04	2.4	-2112.0
(14) $H + H + M \rightleftarrows H_2 + M$	1.00E+18	-1.0	0.0
(15) $H + H + H_2 \rightleftarrows H_2 + H_2$	9.20E+16	-0.6	0.0
(16) $H + H + H_2O \rightleftarrows H_2 + H_2O$	6.00E+19	-1.25	0.0
(17) $H + OH + M \rightleftarrows H_2O + M$	2.21E+22	-2.0	0.0
(18) $H + O + M \rightleftarrows OH + M$	4.71E+18	-1.0	0.0
(19) $O + O + M \rightleftarrows O_2 + M$	1.89E+13	0.0	-1788.0
(20) $HO_2 + HO_2 \rightleftarrows H_2O_2 + O_2$	4.20E+14	0.0	11982.0
(20a) $HO_2 + HO_2 \rightleftarrows H_2O_2 + O_2$	1.30E+11	0.0	-1629.0
(21) $OH + OH(+M) \rightleftarrows H_2O_2(+M)$	1.24E+14	-0.37	0.0

low	3.04E+30	-4.63	2049.0
Troe [0.470 100.0 2000.0 1.0E+15]			
(22) $H_2O_2 + H \rightleftarrows HO_2 + H_2$	1.98E+06	2.0	2435
(23) $H_2O_2 + H \rightleftarrows OH + H_2O$	3.07E+13	0.0	4217.0
(24) $H_2O_2 + O \rightleftarrows OH + HO_2$	9.55E+06	2.0	3970.0
(25) $H_2O_2 + OH \rightleftarrows H_2O + HO_2$	2.40E+00	4.042	-2162.0

An important factor affecting the detonation cell size is the mixture equivalence ratio, e.g. rich mixture (high reactivity) produces smaller detonation cell size. Therefore, a hydrogen/oxygen mixture diluted with argon was used to capture the cell with lower computational costs. Argon dilution will decrease the mixture reactivity and result in overprediction of the detonation cell size [14]. The stoichiometric hydrogen/oxygen mixture diluted with argon is $2H_2$: O_2: 7Ar. It is presumed that the diluent Ar substitutes and plays a similar role to N_2 as inert species in the Marinov's reaction mechanism [13].

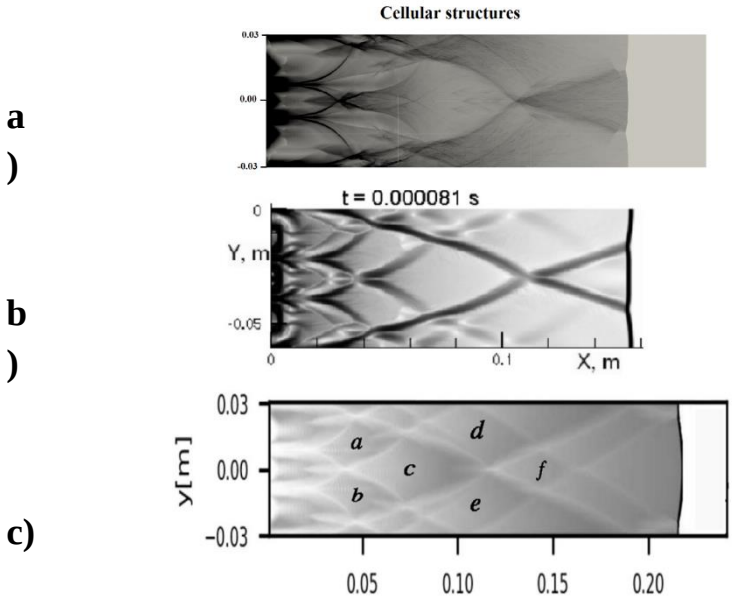

Figure 2. Detonation cellular structure development close to the ignition sources; a) VCEFoam, b) (Kirillov et al., 2005), c) (Marcantoni, Tamagno and Elaskar, 2017)

Figure 2 shows the development of the detonation cellular structure close to the ignition sources. In the present work, the cellular structure has been captured by tracing the triple points in the domain. For tracing triple points, the maximum pressure in each time step of the solution has been stored in memory, and as a result, the cellular pattern could have been captured. In Figure 2 other previous CFD works have been included for comparison. It can be seen that the current captured cellular structure is closer to the previous CFD analysis of Kirillov [15] which can be seen in Figure 2-b.

Table 2: Comparison of cellular structure cell size for H2/Air mixtures.

Reference	α (Cell length)	λ (Cell height)	c^{ar} (aspect ratio λ/α)	Reaction kinetic
Marcantoni et. al [14]	0.074	0.032	0.43	Marinov [13]
Kirillov et. al [15]	0.078	0.033	0.42	Marinov [13]
Eckett [16]	0.054	0.03	0.55	8species/24reactions [20]
Oran et. al [17]	0.055	0.03	0.54	8species/24reactions [20]
Lefebvre & Oran [18]	0.077	0.03	0.42	Two steps model [18]
Lefebvre et. al (Experimental) [19]	0.17	0.09	0.52	smoke foil
VCEFoam (present work)	0.785	0.033	0.0420	Marinov [13]

Table 2 shows a comparison of cellular structure cell size for H2/Air mixtures. In this table, the detonation cell length (α), Cell height (λ, also called cell size), and the cell dimension aspect ratio ($c^{ar} = \lambda/\alpha$), have been provided for different numerical and experimental observations. It can be seen that the predicted cell size of the present work (VCEFoam) are in acceptable agreements with results of Kirillov et al. [15], Marcantoni et al. [14] and Lefebvre & Oran [18]. Note that the numerical setup (boundary and initial conditions) in the present work, is similar to the numerical work done by Kirillov et al. [15] and Marcantoni et al. [14].

The experimental data presented by Lefebvre [19] shows a significant difference in cell size, compared to all the other numerical studies; however, the presented aspect ratio of the experimental observation is close to those given in Refs. [16,17]. One of the possible reasons would be the case that in the experimental observation, due to having a strong ignition source, the first detonation cell was not clear in the shadowgraphs; therefore, the neighbour cell downstream of the tube has been presented. Hence, for further investigation, the same test case has been modelled with tube length extended to 0.5 m.

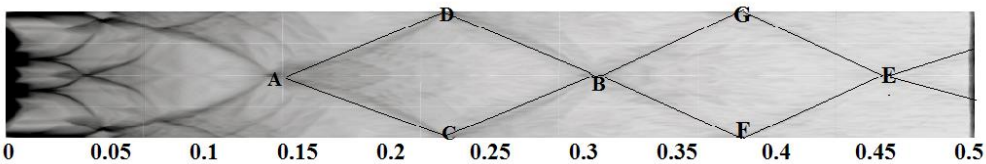

Figure 3. Cellular structure in the extended channel.

The numerical schlieren of the maximum pressure which indicates the cellular structure for the extended channel (to 0.5 m), is presented in Figure 3. In the initial stage, the cellular structure is similar to a shorter channel. However, in the middle of the domain towards downstream two much bigger cell has been (ACBD, and CFEG). These developed cells have a length of $\alpha_{ACBD} = 0.165m$ and $\alpha_{CFEG} = 0.15m$ these are very close to the value presented in the experimental observation ($\alpha_{Experiment} = 0.17m$).
Next, a qualitative comparison of the predicted detonation cell ACBD will be compared with other numerical works as well as an experimental observation.

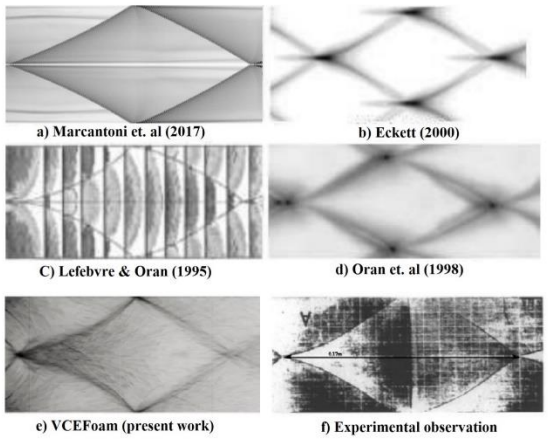

Figure 4. Comparison of Detonation cellular structure.

Figure 4 shows a comparison of detonation cellular structure in hydrogen/air mixture of various other CFD and experimental works. It can be seen that the current captured detonation cell (Figure 4-e), is in good agreement with other past similar works. The captured detonation cell in this study is more similar to the experimental observation as well as the work done by Lefebvre and oran (1995) [18], (Figure 4-c-f).

Figure 5 shows the density distribution of the cellular structure formation process. The evolution of triple points can also be seen in these snapshots. Figure 5 (t=0.688 μs) shows the three ignition areas which act as detonation initiations. Also, in the density snapshot, some small-scale features have been captured, such as forward and backward jets in the detonation fronts which indicates the Richtmyer Meshkov (RM) instability.

Figure 6 shows the numerical schlieren of the maximum pressure distribution of the cellular structure formation process. Also, the evolution of triple points can be seen in these snapshots. It can be seen that the first three perturbations have generated some triple points in the detonation front. Moreover, as a result of a secondary shock collision with the detonation front, a new triple point has been produced (23 μs). The trajectory of the triple points has produced some fish-cell sketches which represent cellular structure. The evaluation of triple points and how they produce a

cellular structure can be found by comparing the numerical schlieren of maximum pressure and the density contours at the same time. At t=0.688 μs, three ignition areas which act as detonation initiations can be found. At 8 μs, three semi-circular detonation fronts propagate downstream and also, as a result of interacting these detonation waves, two critical points (triple points) have been generated on the detonation front. Later, some shock waves reflect from both top and bottom walls before interacting with the other transverse and reflected shocks (at t=23 μs). This interaction of the reflected shock and detonation front will produce an additional triple point. From 29.5 μs onwards it can be seen that the two triple points are moving from top and bottom towards the middle of the domain. At 74.40 μs it can be found that the two triple points meet each other in the middle of the domain, and as a result, another strongly localised detonation occurs. At 90.50 μs it can be seen that two triple points are diverging from the middle and moving towards the top and bottom. Eventually, by tracking these triple points, the trajectory of these points will show "fish-cell" sketches which represent detonation cellular structure.

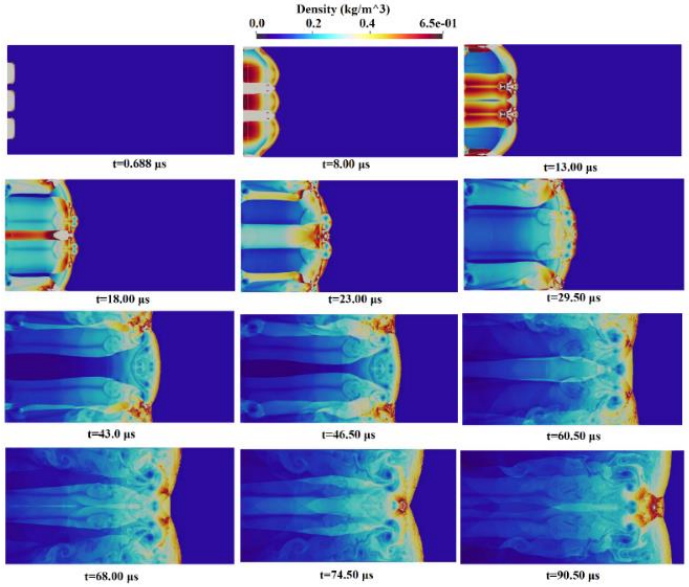

Figure 5. Density distribution: Cellular structure formation process: Evolution of triple points.

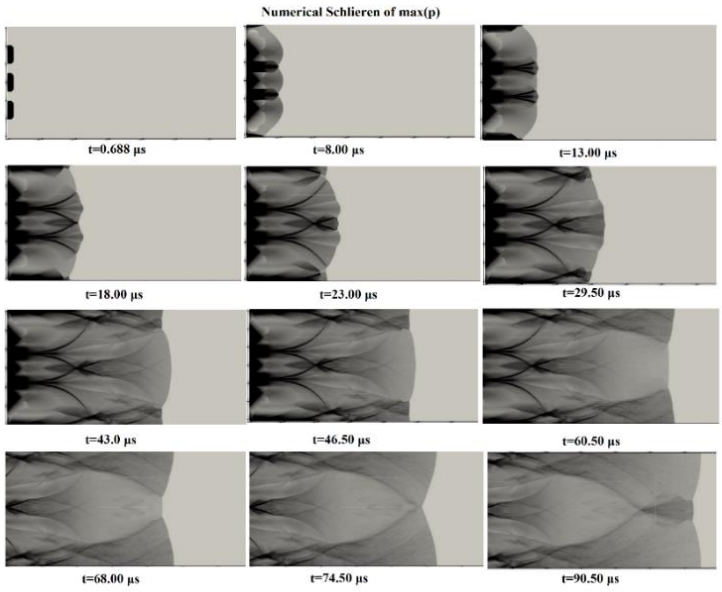

Figure 6. Numerical schlieren of maximum pressure distribution: Cellular structure formation process: Evolution of triple points.

Figure 6 shows the Numerical schlieren of the maximum pressure distribution of the cellular structure formation process. Also, the evolution of triple points It can be seen in this snapshots. It can be seen that the first three perturbation has generated some triple points in the detonation front. Also, it can be found that as a result of a secondary shock collision with detonation front, a new triple point has been produced (23 µs). The trajectory of the triple points has produced some fish-cell sketch which represents cellular structure. The evaluation of triple points and how they produce a cellular structure can be found by comparing the numerical schlieren of maximum pressure and the density contours at the same time. At t=0.688 µs, can be found that there are three ignition areas which act as detonation initiations. At 8 µs it can be seen that three semi-circular detonation front propagates toward downstream and also, as result of interacting these detonation waves, two critical points (triple points) have been generated on the detonation front. In later time, some shock wave reflects from both top and bottom walls, and then they will interact with the other transverse and reflected shock (at t=23 µs). This interaction of the reflected shock and detonation front will produce an additional triple point. From 29.5 µs onwards it can be seen that the two triple points are moving from top and bottom towards the middle of the domain. At 74.40 µs it can be found that the two triple points meet each other in the middle of the domain, and as results, another strongly localised detonation has occurred and at 90.50 µs can be seen that two triple points are diverging from the middle and moving towards top and bottom. Eventually, by tracking these triple points, the trajectory of these points will show a "fish-cell" sketches which represent cellular detonation structure.

4. Quantitative comparison

The experiments of Boeck et al. [8] involving inhomogeneous and homogeneous DDT phenomena of hydrogen-air mixtures were chosen for quantitative validation in the present study. The experiments were conducted in a horizontal obstructed channel with 60% blockage ratios as well as a smooth channel without obstruction. The channel was 60 mm high, 5.4 mm long and 300 mm wide, respectively. The concentration gradients are in the vertical direction. Four sets of the data were used:

1. A homogenous mixture of 30 % H2 (BR60 and BR00).
2. An inhomogeneous mixture of 30 % H2 (BR60 and BR00)

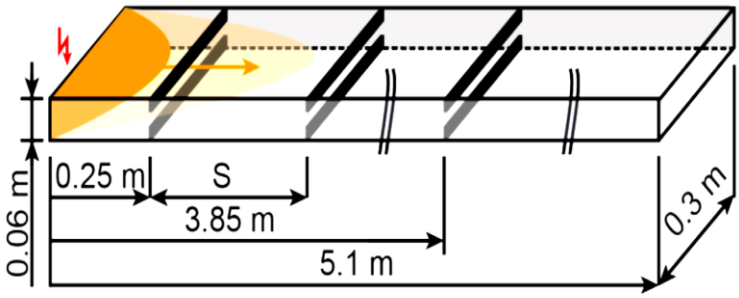

Figure 7. Schematic of the computational domain (Reproduced from [8]).

Figure 7 shows the computational domain which represents a smooth closed channel with obstacles. The mixture was initially in ambient pressure and temperature. In order to initiate ignition, a patch of cells within a radius of 10 mm around the point of ignition (x=0, y=0.03m) was set with a temperature of 2300 K and atmospheric pressure. The half-reaction length of hydrogen changes by equivalence ratio. Moreover, the minimum length is belonging to the stoichiometric value. Therefore, using an adaptive mesh refinement method provided the minimum cell size of 10 µm, giving approximately by average minimum 30 grid points per half reaction length (HRL) in the finest region near the flame and shock fronts.

As shown in Figure 8, the predicted flame position and flame tip speed are in reasonably good agreement with the measurements [8] for the 30 percent hydrogen concentration. For both the homogeneous and inhomogeneous mixtures, the flame velocity rises continuously in the obstructed part of the channel due to flame interaction with the obstacles, resulting in combustion-induced expansion and turbulence generation. Moreover, it can be seen that in the 30 % hydrogen concentration, the homogeneous and inhomogeneous mixture of hydrogen/air, are almost having the same trend of flame acceleration and transition to detonation.

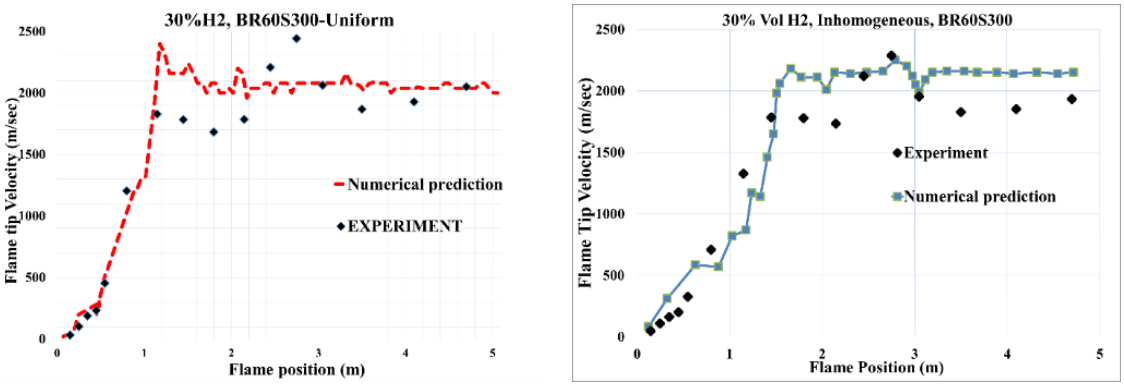

Figure 8. Comparison of between the predicted and measured the flame tip speed in the 30% hydrogen concentration; left: homogenous mixture of hydrogen/air; right: Inhomogeneous mixture of hydrogen/air

Figure 9, shows the predicted temperature contour around the last obstacle (x=2.05 m), where the flame has been fully detonated. At the time 8.0587ms the planner flame ahead with a leading shock interacts to the obstacle and as a result, two reflected shock waves generated in the flame front. Then these reflected shock waves interact in the middle of the channel which leads to a strong shock focusing. In 8.0660 ms can be found that a shear layer has been generated in the reflected detonation wave as a result of the strong shock focusing in the middle of the obstacle. In 8.0702 ms, mushroom shape Jets have generated in the shear layer, which illustrates the existing of Richtmyer- Meshkov (RM) instability. Moreover, the forward jet and backwards jets which are a mushroom form flow, represent the RM instability on the interface between the burned and unburned gas. The forward jets were found to impact on the shock front causing the appearance of a secondary triple point on the initial Mach stem on the flame front. Also, in 8.0828 ms, can see that the leading detonated flame interacts to the upper and lower walls and as result secondary reflected shock wave interacts the downstream of the flame. These shock-flame interacting cause a secondary shear layer in the flame with some small vortices which represent the existing of Kelvin-Helmholtz (KH) instability.

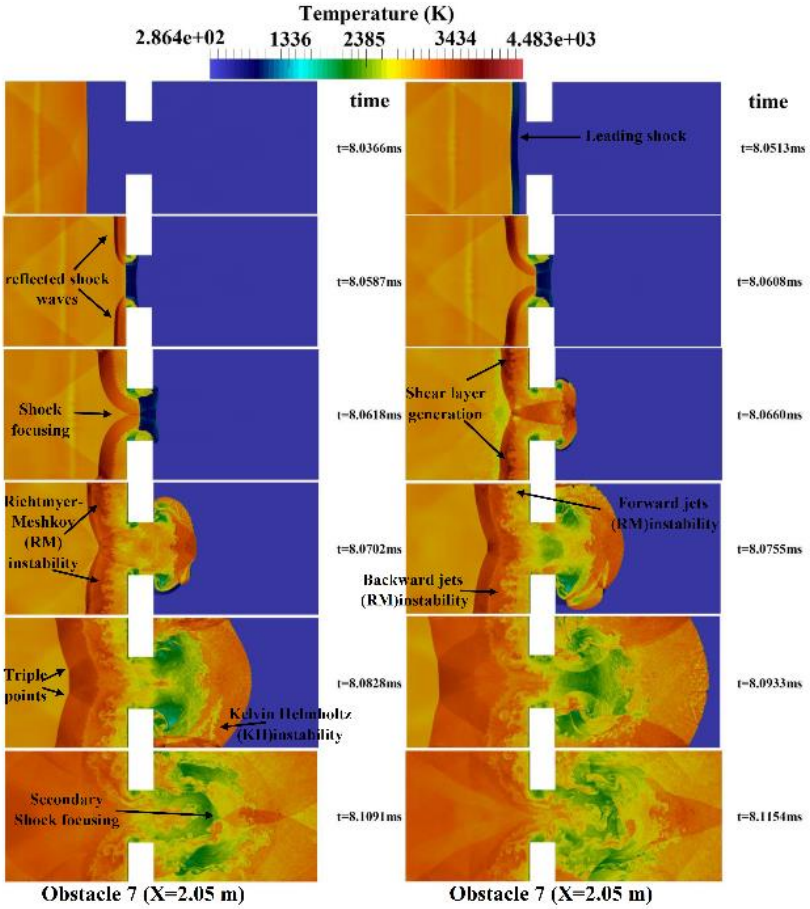

Figure 9: predicted temperature contour in the uniform mixture of 30% hydrogen concentration

Figure 10 shows the pressure and temperature fields produced from the predictions for the case with 30% inhomogeneous mixture of hydrogen/air. In the experiments [8], DDT was initiated by precursor shock reflection at the upstream faces of an obstacle, leading to local explosions behind the reflected shock wave and the onset of detonation either directly from the local explosions or secondary hot-spots downstream of the obstacle. In the homogeneous mixture onset of detonation has got a regular detonation front, while in the inhomogeneous mixture the detonation structure is irregular.

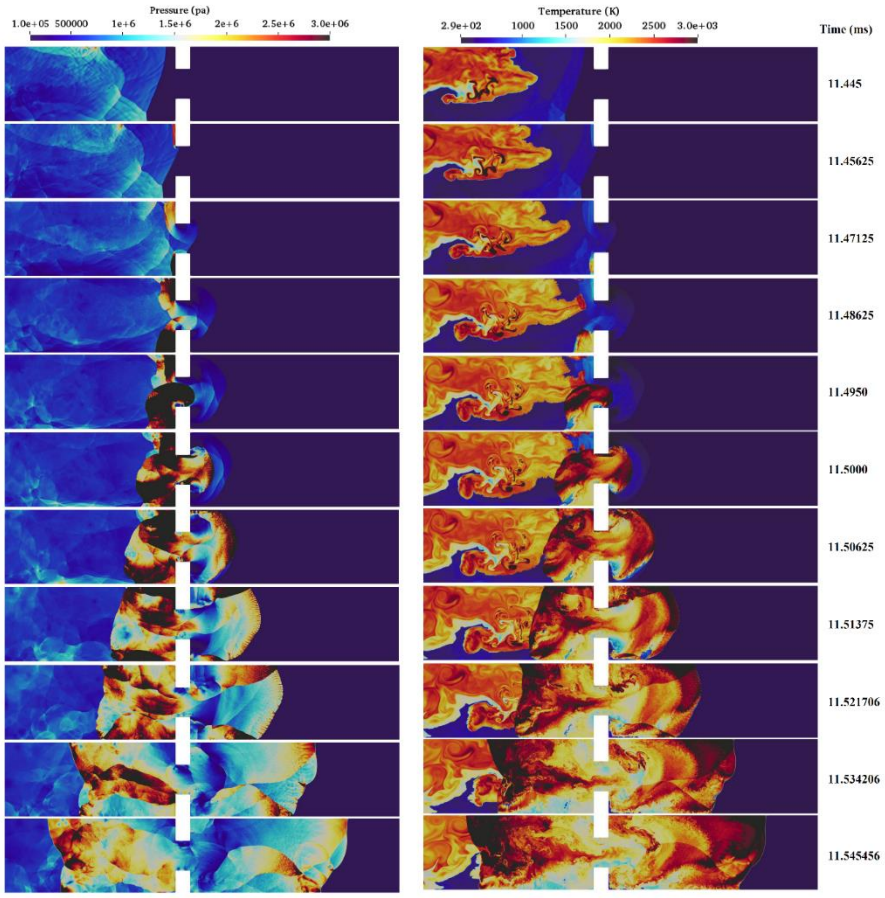

Figure 10: The predicted pressure (left) and temperature fields for the inhomogeneous with 30% hydrogen concentration. The obstacle in the field of view (FOV) is located at x=1.45 m.

Figure 11 shows the onset of detonation in both homogeneous and inhomogeneous mixture of 30% hydrogen/air. Based on figure 6, can be found that in the homogeneous mixture the detonation front is regular however in the inhomogeneous case, the detonation front is irregular, and even the location of triple points is different in these two mixtures. These can be due to having a difference in induction time for the inhomogeneous mixture, rather than the homogeneous case which everywhere the induction times are equal everywhere in the channel.

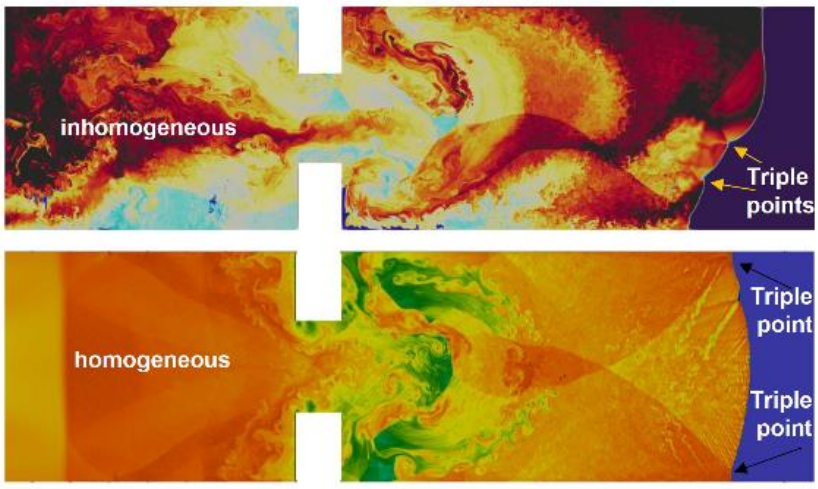

Figure 11. Temperature fields for comparison of onset of detonation, between the inhomogeneous and homogeneous mixture of 30% hydrogen-air.

5. Conclusion

A Numerical model have been developed for flame acceleration and transition to detonation in a horizontal obstructed channel filled with hydrogen/air mixture. DDT test case has been modelled to study the comparison between pressure-based and density-based solution methods. The density-based solver within the OpenFOAM CFD toolbox developed by the present authors [1] is used. High-resolution grids are facilitated by using adaptive mesh refinement technique, which leads to 30 grid points per half reaction length (HRL) in the finest region near the flame and shock fronts. In the detonation initiation test case the capability of the current numerical code in capturing the detonation cellular structure has been examined. A small test case has been modelled with using three high ignition point to produce detonation initiation. The CFD results have been compared against both quantitatively and qualitatively with the other previous works as well as an experimental observation. Overall, the predicted flame tip velocities, overpressures, and locations of detonation onset are in reasonably good agreement with the measurements. For both uniform and non-uniform mixtures with 30% hydrogen concentration, the onset of detonation occurs within the obstructed channel section, but the homogeneous mixtures show slightly faster flame acceleration and earlier onset. The captured detonation cell size was in good agreement with the other CFD works and the experimental observations. Furthermore, it has been found that the non-uniform mixtures cause higher shock and flame velocities compared to the uniform mixtures concentration.

References

[1] Khodadadi Azadboni R, Heidari A, Wen JX. (2018). Acomputational fluid dynamic investigation of inhomogeneous hydrogen flame acceleration and transition to detonation. Turbulence and Combustion, Flow, 101:1009–1021.
[2] Lee JHS. (1977). Initiation of gaseous detonation. Ann. Rev. Phys. Chem. 28: 75.
[3] Teodorczyk A. (2008). Scale effects on hydrogen-air fast deflagrations and detonations in small obstructed channels. Journal of Loss Prevention in the Process Industries, 21(2):147–153.
[4] Frolov SM. (2012). Acceleration of the deflagration-to-detonation transition in gases: From Shchelkin to our days. Combustion, Explosion, and Shock Waves, 48(3):258–268.
[5] Gamezo VN, Ogawa T, & Oran ES. (2007). Numerical simulations of flame propagation and DDT in obstructed channels filled with hydrogen-air mixture. Proceedings of the Combustion Institute 31: 2463–2471.
[6] Kuznetsov MS, Grune J, Friedrich A, Sempert K, Breitung W, and Jordan T. (2011). Hydrogen-Air Deflagrations and Detonations in a Semi-Confined Flat Layer. In Sixth International Seminar on Fire and Explosion Hazards, pages 978–981.
[7] Vollmer KG, Ettner F, Sattelmayer T. (2012). Deflagration-to detonation transition in hydrogen-air mixtures with a concentration gradient. Combust Sci Technol. 184:1903-1915.
[8] Boeck LR, Katzy P, Hasslberger J, Kink A, Sattelmayer T. (2015). The "GraVent DDT Database". 25th International Colloquium on the Dynamics of Explosions and Reactive Systems (ICDERS), Leeds, UK.
[9] OpenFOAM Ltd., OpenFOAM, Available from: http://www.openfoam.com/.
[10] O'Conaire M, Curran H, Simmie J, Pitz W, Westbrook C. (2004). A comprehensive modeling study of hydrogen oxidation. Int J Chem Kinet. 36:603-622.
[11] Khodadadi Azadboni R, Heidari A, Wen JX. (2017). Numerical modeling of flame acceleration and transition from deflagration to detonation using OpenFOAM. In J. Miguel Nóbrega, Hrvoje Jasak eds., "OpenFOAM®: Selected papers of the 11th Workshop", Springer, 11 Dec. 2018. ISBN: 9783319608457.
[12] Khodadadi Azadboni R, Wen JX, Heidari A, Wang CJ. (2017). Numerical modeling of deflagration to detonation transition in inhomogeneous hydrogen/air mixtures. J of Loss Prevention in the Process Industries. (49) 722-730.
[13] Marinov N, Westbrook C, Pitz W. (1996). Detailed and global chemical kinetics model for hydrogen-air. Vol. 8 of International Symposium on Transport Properties, Lawrence Livermore National Laboratory. p. 118.
[14] Marcantoni LFG, Tamagno J, Elaskar S. (2017). Two-dimensional numerical simulations of detonation cellular structures in H2-O2-Ar mixtures with OpenFOAM. International journal of hydrogen energy, 42, pp: 26102-26113.
[15] Kirillov I, Strelkova M, Panasenko A, Roekaerts D. (2005). Sensitivity to detonation and detonation cellular structure of H2-O2-air-H2-O2 gas mixtures. In: First int. Conference on hydrogen safety, Pisa, Italy, p. 8e10.
[16] Eckett CA. (2000). Numerical and analytical studies of the dynamics of gaseous detonations. Ph.D. thesis.

[17] Oran ES, Weber JW, Stefaniw EI, Lefebvre MH, Anderson JD. (1998). A numerical study of a two-dimensional H2-O2-Ar detonation using a detailed chemical reaction model. Combust Flame.113(1):147e63.http://dx.doi.org/10.1016/S0010-2180(97)00218-6
[18] Lefebvre M, Oran E. (1995). Analysis of the shock structures in a regular detonation. Shock Waves, 4(5):277e83.
[19] Lefebvre MH, Weber JW, Oran ES. (1997). Numerical simulations of a marginal detonation: wave velocities and transverse wave structure. In: IUTAM symp. on combust. in supersonic flows. Springer. p. 347e58.
[20] Burks TL, Oran ES. (1981). A Computational Study of the Chemical Kinetics of Hydrogen Combustion. Naval research lab Washington DC.